

AMM003

# Real-time Observation of Small Fatigue Crack Growth in Type 329J4L Duplex Stainless Steel using High-Resolution Digital Microscope

Keisuke Tsuchida<sup>1</sup>, Yoshihiko Uematsu<sup>2,\*</sup>, Toshifumi Kakiuchi<sup>2</sup>, Masayuki Akita<sup>3</sup>, and Masaki Nakajima<sup>4</sup>

<sup>1</sup> Graduate School of Engineering, Gifu University, 1-1 Yanagido, Gifu, 501-1193, Japan

<sup>2</sup> Department of Mechanical Engineering, Gifu University, 1-1 Yanagido, Gifu, 501-1193, Japan

<sup>3</sup> Faculty of Engineering, Gifu University, 1-1 Yanagido, Gifu, 501-1193, Japan

<sup>4</sup> National Institute of Technology, Toyota College, 2-1 Eiseicho, Toyota, Aichi, 471-8525, Japan

\* Corresponding Author: yuematsu@gifu-u.ac.jp, +81-58-293-2501, +81-58-293-2491

## Abstract

Rotating bending fatigue tests had been conducted using type 329J4L duplex stainless steel, and small fatigue crack initiation and growth behavior was continuously monitored by both plastic replication method and high-resolution digital microscopic observation. In the plastic replication method, a fatigue test was periodically terminated and surface profile was replicated to a plastic film during the termination. By digital microscopic observation, fatigue crack initiation and growth were directly and continuously monitored without termination of fatigue test, namely real-time observation of fatigue crack. Fatigue crack initiation lives and growth rates were compared between conventional plastic replication and digital microscopic methods. Fatigue crack initiation lives and crack growth rates corresponded well between those two methods. However, the smallest crack size detected by a digital microscope was slightly larger than that by a plastic replication. The lower resolution of the smallest fatigue crack found by a digital microscope could be attributed to the vibration of fatigue specimen during real-time observation.

**Keywords:** Fatigue, Crack initiation, Crack growth, Plastic replication, Real-time observation

## 1. Introduction

Fatigue life of structural material could be classified into two regions, namely crack initiation and crack growth lives. Furthermore, it is well known that small fatigue crack grows faster than long crack, when the crack growth rates were evaluated using conventional Paris law ( $da/dn = C\Delta K^m$ ,  $a$ : crack length,  $n$ : number of cycles,  $\Delta K$ : stress intensity factor range,  $C$  and  $m$ : material's constants) [1]. Consequently it is important to monitor fatigue crack initiation and small fatigue crack growth from the view point of structural reliability. A plastic replication technique has been widely used for the monitoring of fatigue crack, in which fatigue test was periodically terminated and surface profile was replicated to a plastic film during the termination. By a plastic replication method, fatigue crack initiation life and small crack growth rates were well estimated in many structural materials [2-4]. In this method, however, temporary stoppings of fatigue test are inevitable. It implies that this method is quite time-consuming, and real-time observation of growing fatigue crack is not possible due to the termination.

In the present study, rotating bending fatigue tests had been conducted using type 329J4L duplex stainless steel, and small fatigue crack initiation and growth behavior were continuously monitored using a high-resolution digital microscope. Fatigue crack initiation lives and growth rates were compared between conventional plastic replication and digital microscopic methods.

## 2. Experimental Procedure

### 2.1 Material and specimen

The material used in this study is type 329J4L duplex stainless steel. The round-bar material with the diameter,  $\phi=16\text{mm}$  was solution treated at  $1080^\circ\text{C}$  followed by water quenching. The chemical composition is as follows; C: 0.019, Si: 0.52, Mn: 0.68, P: 0.032, S: <0.001, Ni: 6.68, Cr: 25.37, Mo: 3.04, N: 0.014, Fe: bal. (mass.%). The mechanical properties of the material were obtained using tensile specimen configuration in accordance with JISZ2201. The results are as follows; tensile strength ( $\sigma_B$ ): 766MPa, 0.2% proof stress ( $\sigma_{0.2}$ ): 642MPa, Elastic modulus ( $E$ ): 142GPa, Elongation ( $\delta$ ): 26%, Reduction of area ( $\phi$ ): 83%.

The microstructure of the material is revealed in Fig. 1, consisting of  $\alpha$  (ferritic) and  $\gamma$  (austenitic) phases. The phase ratio of  $\alpha$  and  $\gamma$  is 7:3. Rotating bending fatigue specimen was cut from the solution-

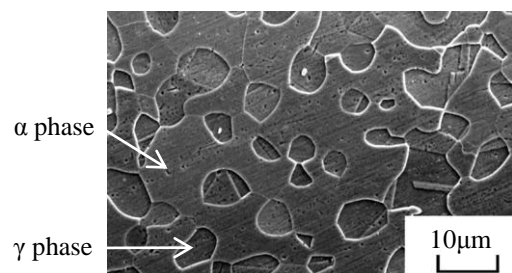


Fig. 1 Microstructure of type 329J4L duplex stainless steel.

# AMM003

treated round bar, and the specimen configuration is shown in Fig. 2.

## 2.2 Fatigue testing procedure

Fatigue tests were conducted using a cantilever-type rotating bending fatigue testing machine in laboratory air. Test frequency,  $f$ , was 20Hz.

Fatigue crack initiation and growth behavior were monitored by plastic replication and high-resolution digital microscopic methods. In the plastic replication method, a fatigue test was periodically terminated. Specimen surface morphology was replicated to a plastic film at each termination. The replication films were observed in detail using an optical microscope. In the digital microscopic method, another fatigue test was conducted at the same stress amplitude without any termination of the fatigue test. The specimen surface of the narrowest area in the specimen configuration (Fig. 2) was continuously monitored using a high-resolution digital microscope. The recording conditions are summarized in Table 1. The zoom-lens with the long focus and magnification of 400 times was mounted on the specimen. The specimen surface was observed in real-time, and the moving image was stored in the hard disc with the frame rate, 200fps, and resolution 640×480 pixel. The shutter speed was set to be 1/40000sec.

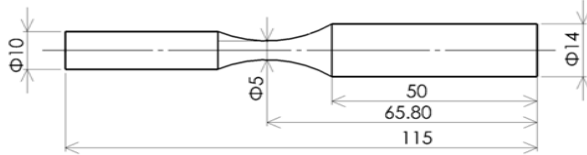


Fig. 2 Fatigue specimen configuration.

Table. 1 Recording conditions.

Magnification	400 times
Shutter speed	1/40000 sec
Frame rate	200 fps
Resolution	640×480 pixels

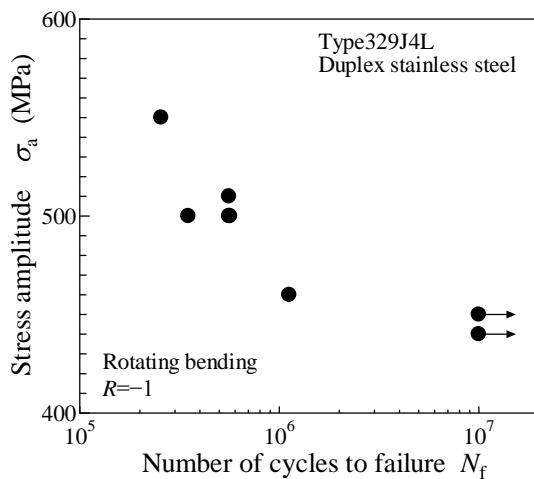


Fig. 3 S-N curve of type 239J4L.

## 3. Results and Discussion

### 3.1 Fatigue strength

The  $S-N$  curve of the material is shown in Fig. 3. The fatigue limit was defined as the stress amplitude at the run-out cycle of  $10^7$ . In this case, the fatigue limit was defined as 450MPa. When the stress amplitude,  $\sigma_a$ , is 500MPa, the number of cycles to failure,  $N_f$ , would be about  $5 \times 10^5$  cycles according to the  $S-N$  curve. Consequently, two fatigue tests were conducted at the stress amplitude of 500MPa, and one test was monitored by a plastic replication method and the other was by a digital microscope. Figure 4 reveals fracture surface near the crack initiation site at  $\sigma_a=510$ MPa ( $N_f=5.6 \times 10^6$ ). In very hard steels, sub-surface crack initiation is dominant in high cycle region [5]. But the Vickers hardness of type 329J4L was measured as about 300HV, and not too hard to show sub-surface crack initiation. Consequently, surface crack initiation was dominant at all stress levels as shown in Fig.4.

### 3.2 Time-series observation of fatigue crack

Figure 5 shows the typical images of plastic replicas observed by an optical microscope. It should

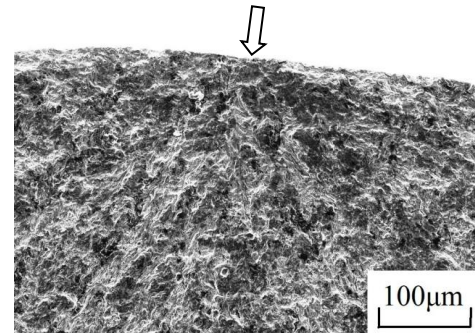


Fig. 4 SEM micrograph showing crack initiation site ( $\sigma_a=510$ MPa,  $N_f=5.6 \times 10^6$ ). Arrow indicates crack initiation site.

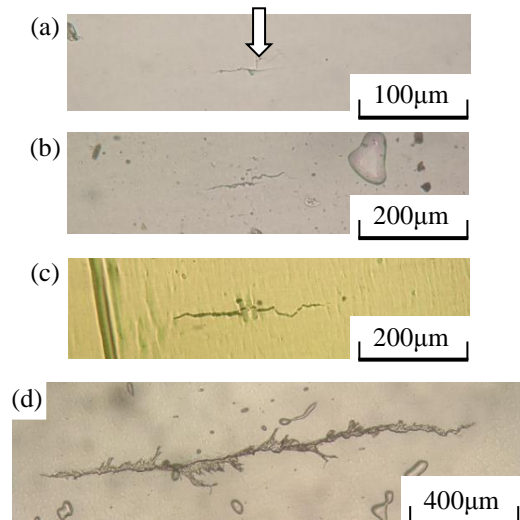


Fig. 5 Time-series observation of fatigue crack by a plastic replication method; (a)  $N=2.2 \times 10^5$ , (b)  $N=3.6 \times 10^5$ , (c)  $N=4.3 \times 10^5$ , (d)  $N=5.3 \times 10^5$ .

## AMM003

be noted that the smallest crack with the size of about  $50\mu\text{m}$  was found at the number of cycles,  $N$ , of  $2.2 \times 10^5$  as revealed in Fig. 5(a). It was confirmed that the fatigue crack stably grew during fatigue test. The real-time observation results of fatigue crack by a digital microscope are shown in Fig. 6. Stable crack growth was successfully observed in real time by a digital microscope. But the smallest crack identified at the initial stage was about  $90\mu\text{m}$  at  $N=2.2 \times 10^5$  (Fig. 6(a)), and that was longer than that observed by a plastic replication method (Fig. 5(a)).

### 3.3 Quantitative analyses of fatigue crack

Crack length,  $2c$ , on the specimen surface was plotted as a function of number of cycles,  $N$ , in Fig. 7. In this case, the crack was projected in a loading direction, and defined as the projected length. It is clear from the figure that the fatigue crack stably grew until final fracture. From this figure, crack growth rates,  $da/dN$ , could be calculated using tangents of the curves. However, fatigue lives are slightly different in both curves in spite of the same stress amplitude of 500MPa. This difference could be attributed to the

scatter of material. Thus, crack length was replotted as a function of cycle ratio,  $N/N_f$ , where  $N_f$  is number of cycles to failure. As shown in Fig.8, the shapes of two curves correspond well, indicating that the crack length was successfully monitored by a high-resolution digital microscope. The crack was detected at  $N/N_f=0.39$  by a plastic replication method, but at  $N/N_f=0.6$  by a digital microscope, because a plastic replication method has a higher resolution for finding small crack. But it should be noted that the digital microscopic observation was performed in real time, and the actual operation time was much shorter than a plastic replication method.

Subsequently, fatigue crack growth rates,  $da/dN$ , were calculated from Fig. 7 and plotted in terms of maximum stress intensity factor,  $K_{\text{max}}$ , as revealed in Fig. 9. Stress intensity factor of rotating bending specimen was calculated based on Murakami's equation [6]. As shown in Fig. 9,  $da/dN$ - $K_{\text{max}}$  relationship estimated from digital microscopic observation is in accordance with that based on a

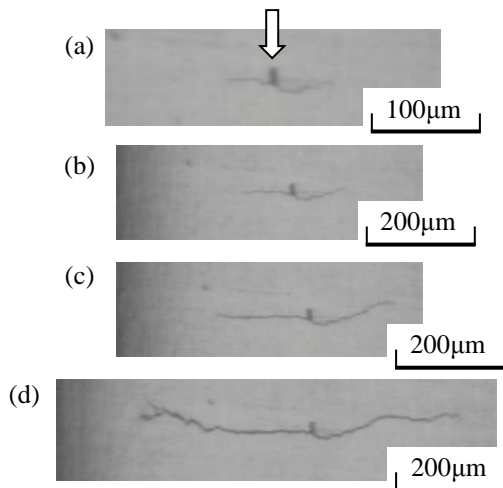


Fig. 6 Real-time observation of fatigue crack by a digital microscope; (a)  $N=2.2 \times 10^5$ , (b)  $N=2.4 \times 10^5$ , (c)  $N=2.7 \times 10^5$ , (d)  $N=3.0 \times 10^5$ .

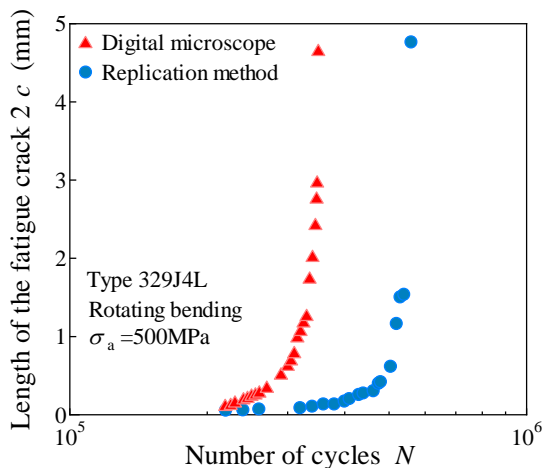


Fig. 7 Crack lengths,  $2c$ , as a function of number of cycles,  $N$ .

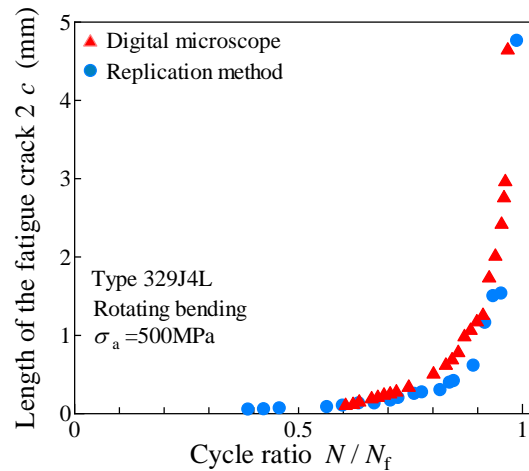


Fig. 8 Crack lengths,  $2c$ , as a function of cycle ratio,  $N/N_f$ .

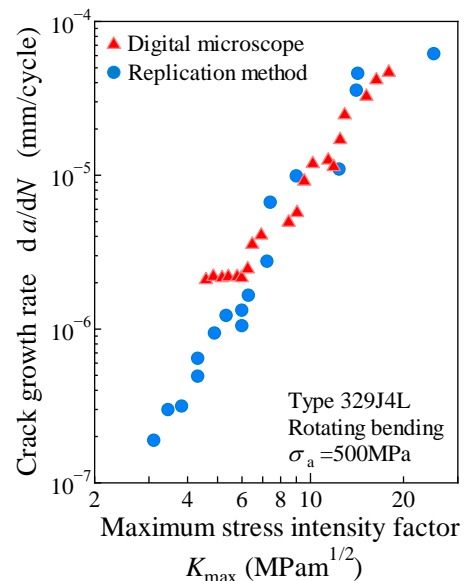


Fig. 9 Relationship between crack growth rate,  $\Delta K$ , and maximum stress intensity factor,  $K_{\text{max}}$ .

**AMM003**

plastic replication method. Due to the limitation of the resolution of initial crack,  $da/dN-K_{max}$  relationship estimated from digital microscopic observation starts at higher  $K_{max}$  value than a plastic replication method.

**3.4 Accuracy of real-time observation**

To estimate the accuracy of real-time observation using a digital microscope, one fatigue test was conducted at the stress amplitude of 500MPa, and the same crack was monitored by both plastic replication method and digital microscopic observation. The cracks observed by both methods are shown in Fig. 10. And the crack lengths identified by both methods are summarized in Table 2. The shapes of the cracks are nearly the same at each stage shown in Fig. 10. Furthermore, the difference of crack lengths between those methods is quite small (see Table 2).

Consequently, it was proved that the high-resolution digital microscope was very effective for real-time fatigue crack observation, and crack length analyses. However, the resolution of the initial crack was still better in a plastic replication method. The lower resolution of finding small crack in a digital microscopic method could be attributed to the vibration of the specimen during real-time observation. Thus some image stabilization technique should be integrated to improve the resolution in real-time observation using a digital microscope.

**4. Conclusions**

Rotating bending fatigue tests had been conducted using type 329J4L duplex stainless steel. Fatigue specimen surface was investigated by a plastic replication method and digital microscopic observation

to investigate fatigue crack initiation and growth behavior. The observation results obtained by both methods were compared. The conclusions are as follows.

1. Basic  $S-N$  curve was obtained by the fatigue tests, revealing the fatigue limit of 450MPa. Based on the fractographic analyses, it was confirmed that surface crack initiation was dominant at all tested stress amplitudes.
2. Crack length was successfully monitored by a high-resolution digital microscope. The crack growth curves in terms of  $N/N_f$  obtained by both methods were nearly the same.
3.  $da/dN-K_{max}$  relationship estimated by digital microscopic observation corresponded well with that by a plastic replication method, indicating that a digital microscope was effective to reduce time and cost in fatigue crack observation.

Table. 2 Crack length estimated by both digital microscope and plastic replication method.

Number of cycles $N$	Crack length $2c$ ( $\mu\text{m}$ )	
	Digital microscope	Plastic replication
$2.3 \times 10^5$	136	139
$2.5 \times 10^5$	151	145
$2.7 \times 10^5$	163	156
$2.9 \times 10^5$	230	227
$3.1 \times 10^5$	315	306
$3.3 \times 10^5$	486	469
$3.4 \times 10^5$	585	609
$3.5 \times 10^5$	735	734
$3.6 \times 10^5$	953	950
$3.7 \times 10^5$	1312	1295

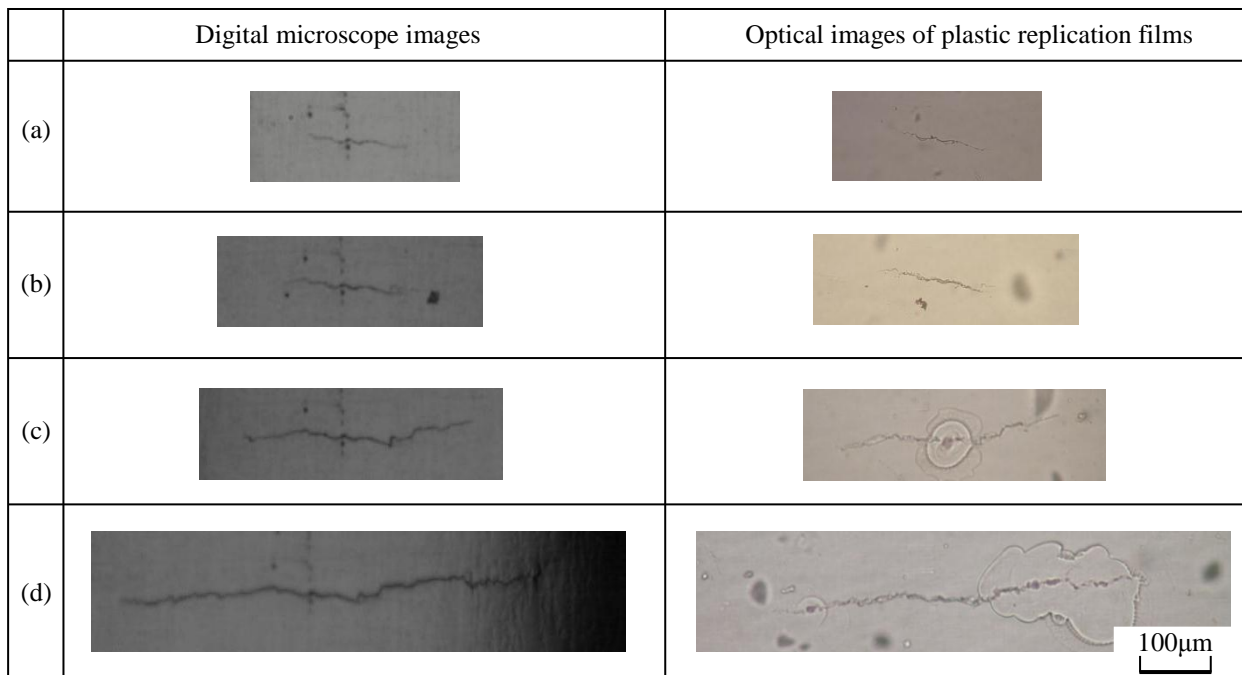


Fig. 10 Comparison of crack shapes between digital microscope and plastic replication; (a)  $N=2.3 \times 10^5$ , (b)  $N=2.7 \times 10^5$ , (c)  $N=3.1 \times 10^5$ , (d)  $N=3.4 \times 10^5$ .

## AMM003

4. The resolution in finding initial crack was better in a plastic replication method. The lower resolution in digital microscopic observation was attributed to the vibration of the specimen during real-time observation.

### 5. References

- [1] Pearson, A. (1975). Initiation of fatigue cracks in commercial aluminium alloys and the subsequent propagation of very short cracks, *Engineering Fracture Mechanics*, vol.7, pp. 235 – 247.
- [2] Uematsu, Y., Akita, M., Nakajima, M. and Tokaji, K. (2008). Effect of temperature on high cycle fatigue behaviour in 18Cr-2Mo ferritic stainless steel, *International Journal of Fatigue*, vol.40(1), January2008, pp. 138 – 141.
- [3] Uematsu, Y., Tokaji, K. and Matsumoto, M. (2009). Effect of aging treatment on fatigue behaviour in extruded AZ61 and AZ80 magnesium alloys, *Materials Science and Engineering: A*, vol.517(1-2), August2009, pp. 138 – 145.
- [4] Akita, M., Nakajima, M., Uematsu, Y., Tokaji, K. and Kojima, T. (2014). High cycle fatigue properties of beta Ti alloy 55Ti-30Nb-10Ta-5Zr, *Gum Metal, Fatigue and Fracture of Engineering Materials and Structures*, vol.37(11), November2014, 1223 – 1231.
- [5] Uematsu, Y., Kakiuchi, T., Maruchi, K., Teratani, T. and Harada, Y. (2011). Effect of DLC film on fatigue behavior in alloy steels with different hardness and inclusion size, *Journal of the Society of Materials Science, Japan*, vol.60(12), December2011, pp.1064 – 1103.
- [6] Committee on Fracture Mechanics The Society of Materials Science, Japan (1987). *STRESS INTENSITY FACTORS HANDBOOK*, vol.2, pp.657 – 658.